Scanning-force-microscopy study of MeV-atomic-ion-induced surface tracks in organic crystals

J. Kopniczky, C. T. Reimann, A. Hallén, and B. U. R. Sundqvist
Division of Ion Physics, Department of Radiation Sciences, Uppsala University, Box 535, S-751 21 Uppsala, Sweden

P. Tengvall and R. Erlandsson
Department of Physics and Measurement Technology, Laboratory of Applied Physics, S-581 83 Linköping, Sweden
(Received 21 July 1993)

We present scanning force microscope images of craterlike defects induced by individual 78.2-MeV ^{127}I ions incident on organic single-crystal *L*-valine surfaces. For grazing incidence ions, the craters are elongated along the ion azimuth of incidence and display a raised tail in the surface above the ion track. This permanent plastic deformation of the surface indicates that a hydrodynamic pressure-pulse phenomenon occurs in response to the electronically deposited energy.

Ionizing radiation is important in nature. For example, tracks from solar emissions are found in interplanetary dust,[1] and α-particle irradiation may cause chromosomal aberrations in cells.[2] Motivated both by fundamental and practical considerations, studies of nuclear tracks in solids have been carried out for many years.[3] Here we consider the special case of electronic excitation of insulating organic matter by energetic heavy atomic ions. Such ions cause severe damage to fragile biomolecules located within a distance ≈ 3 nm from the ion track.[4] Surprisingly, sputtering yields of the order of $\approx 10^3$ intact, neutral molecules per incident ion are measured,[4] and the intact molecular-ion yield is useful in mass spectrometic applications.[5] The field of sputtering of organic solids has recently been reviewed.[6,7]

Ejection of an intact organic molecule requires two special conditions. First, the momentum of the desorbed molecule must be large owing to the large mass.[8] Second, the internal vibrational modes must not be in thermal equilibrium with the translational mode.[8-10] Hydrodynamical or continuum-mechanical models have been proposed that satisfy these conditions.[11] For each ion impact, a pressure pulse[12-14] or a shock wave[15] emanates from the ion track, producing a correlated volume force on a block of molecules and causing intact ejection. However, thermal evaporation may also be an effective sputtering mechanism if the coupling of energy into vibrational modes of the desorbed species is inefficient.[10] In order to obtain new information which might clarify the sputtering mechanism, craterlike defects induced by ions incident on the surfaces of single-crystal amino acid *L*-valine were investigated by scanning force microscopy (SFM). The results presented here seem to be the first observations of topographical defects induced in organic solids by individual incident heavy energetic atomic ions.

L-valine (MW 117 u, Sigma Chemicals) was dissolved in deionized water to near saturation (80–100 %). Droplets of the solution were placed on silicon plates and evaporated, producing molecularly flat crystals oriented exposing the [100] face.[16] Samples were bombarded by charge-equilibrated 78.2-MeV ^{127}I ions from the Uppsala EN-tandem van de Graaff accelerator (stopping cross section ≈ 66.7 MeV mg^{-1} cm^2). The areal density of observed surface defects was approximately in agreement with the estimated fluence of ions incident on the samples. SFM studies were performed under ambient conditions. A TopoMetrix-2000 (TopoMetrix Corp., Santa Clara, CA) was employed in the conventional continuous contact mode. The tips employed have a radius of curvature ≈ 10 nm and cone angle $< 6°$. The net force on the tip was $\approx 0.1-1.0$ nN, but the surface contact force was much higher due to strong capillary attraction between the tip and a contamination layer. Consequently, strong lateral frictive forces occurred during scanning. A NanoScope III (Digital Instruments, Santa Barbara, CA) was employed in a newly available large-amplitude-oscillating intermittent contact or tapping mode. In this mode, the tip is oscillated with an amplitude of ≈ 100 nm and a frequency of 330 kHz. The cantilever spring force at contact counteracts the strong capillary force so that surface contact forces as low as 0.1 to 1 nN may be employed (personal communication, Digital Instruments). Also, lateral forces during scanning are sharply reduced relative to those present in the conventional continuous contact mode. The tip in the tapping mode has a radius ≈ 10 nm and cone angle 36°.

Typical SFM images taken in the continuous contact mode are shown in Figs. 1 and 2. Samples bombarded at normal incidence show holes of diamter ≈ 17 nm and depth ≈ 0.4 nm (Fig. 1). Increasing the net force on the stylus by a factor of 10 causes the diameter and depth of craters to increase by $\sim 16\%$ and $\sim 75\%$, respectively. For a grazing angle of incidence 79°, craters display diameter ≈ 30 nm and depth ≈ 1.6 nm (Fig. 2). A raised tail of height 1 nm and width 89 nm appears behind each crater, oriented precisely in the direction of the azimuth along which the incident ion penetrates the surface. The tail length increases for more grazing angles of incidence, up to a maximum of 300 nm. The craters are distorted in the stylus scanning direction and can be altered by repeated scanning. It is likely that the surface undergoes significant distortion during SFM imaging in the continu-

0163-1829/94/49(1)/625(4)/$06.00

FIG. 1. Continuous contact mode SFM image of single-crystal L-valine irradiated at normal incidence by 78.2-MeV ^{127}I ions. Some distortion due to tip-surface interactions is apparent.

ous contact mode.

Typical images acquired in the tapping mode are shown in Figs. 3 and 4. Samples bombarded at normal incidence show holes ≈ 16 nm in diamter and ≈ 0.3 nm deep (Fig. 3). The craters seem to display ≈ 0.1-nm-tall rims. Occasionally, bumps of width ≈ 15 nm and height ≈ 0.3 nm are observed, suggesting incomplete crater formation. Images are reproducible to within $\approx 30\%$ under multiple scanning. Under grazing incidence (Fig. 4), observed craters are typically ≈ 92 nm wide, ≈ 155 nm long, and ≈ 12 nm deep. The tails are ≈ 150 nm wide, ≈ 1100 nm long, and ≈ 1.1 nm high. Sometimes a ≈ 14-nm-tall and ≈ 220-nm-long amorphous bulge appears between the crater and the tail.

Metrology of craters and bumps in the size range studied here and on such soft samples clearly presents a challenge for SFM technology. Sizable differences exist between results obtained with continuous contact and tapping modes of SFM which cannot be explained in terms of tip convolution effects,[17] but which may instead be attributable to the lower effective tip loading force when using the tapping mode. It is possible that spatially localized variations in surface elasticity could create imaging

FIG. 2. Continuous contact mode SFM image of single-crystal L-valine irradiated at a 79° grazing angle of incidence. The tail is smooth as evidenced by the preserved step edge seen crossing one of the tails.

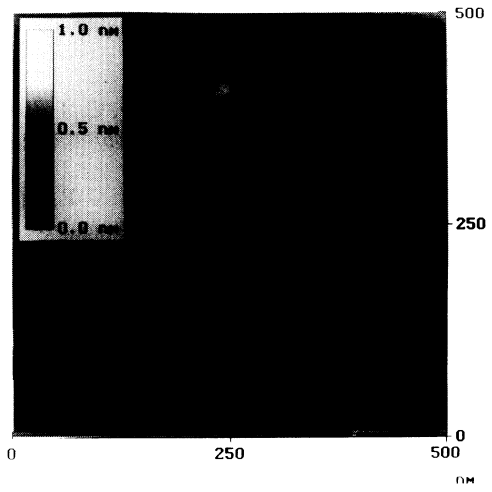

FIG. 3. Tapping mode SFM image of single-crystal L-valine irradiated at normal incidence.

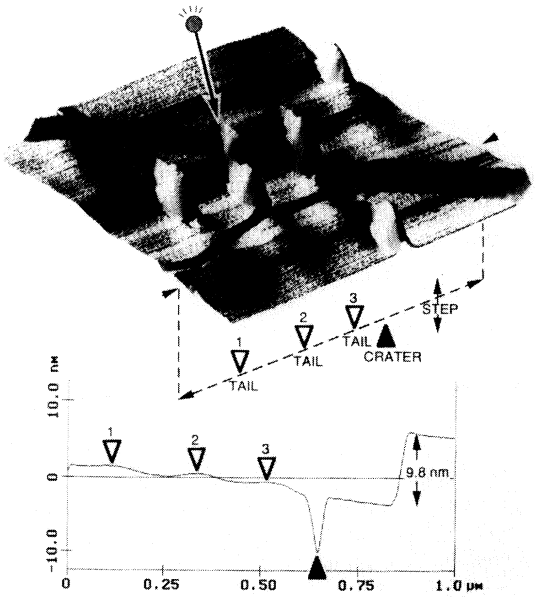

FIG. 4. Tapping mode SFM image of single-crystal L-valine irradiated at grazing incidence. The direction of the incident ions is shown schematically (note that the vertical scale differs from the horizontal scale). The scan area is 1000 nm × 1000 nm. The dominant step edge is 9.8 nm tall and corresponds closely to eight crystal planes (Ref. 16). A profile scan of three of the tails is shown.

artefacts, as could preferential adsorption of contaminants at the ion impact sites. The consistent observation of subfeatures of inverse curvature in close proximity (e.g., craters versus rims and raised tails) in two different SFM imaging modes seems to rule out this possibility. Although quantification of our SFM images is difficult, we obtain qualitative information on the topography of the defects.

Our results may be compared with the results of previous studies. Impact features induced in gypsum by grazing incidence 100-MeV ^{132}Xe ions and analyzed by an electron microscope replica method[18] are qualitatively similar to our observations of craters with accompanying raised tails. Other studies have been performed with normally incident ions. In a continuous contact mode SFM study of defects induced in mica by 2.9-GeV ^{84}Kr ions, circular holes were observed and interpreted as soft areas on the surface rather than as topography.[19] Similar conclusions were reached in a study of columnar defects induced in a layered superconductor by 1-GeV ^{208}Pb ions; these defects appeared as regions of higher lateral frictive force on the SFM stylus during scanning.[20] These results are in contrast to ours, in which we observe the topography of defects. Finally, it should be noted that successful attempts have been made to image with SFM etched ion tracks in glass and in organic substances like polycarbonate[21] and mica.[22]

Indirect evidence for cratering in organic solids has been obtained from measurements of desorption of ionic species from layered Langmuir-Blodgett films.[23–25] Since a buried marker layer contributes a measurable desorbed ion signal from as deep as 20 nm, it was concluded that craters of comparable depth are formed. Our results obtained with the tapping mode SFM are in qualitative agreement with this crater depth, at least for grazing incidence ions.

We present a qualitative description of a pressure pulse model[12–14] to describe our observations. For normal incidence (Fig. 5, top), electronic energy deposited by an incident ion relaxes, depositing kinetic energy into the nuclear system. This may occur via a Coulomb explosion in the heavily ionized track; alternatively, secondary electrons emitted from the track may excite surrounding molecules, causing localized expansion (indicated by the three pulses, Fig. 5, top left). The evolution of the kinetic-energy density in space and time, $\varepsilon(\rho,z,t)$, is governed by a diffusion equation. Evaporation from the surface on a molecule-by-molecule basis, as in a thermal spike, could yield a crater but not a rim. However, $\varepsilon(\rho,z,t)$ displays a gradient, which is equivalent to a force per unit volume. If the impulse to a volume of material due to this force exceeds a critical value, and if the escape path is clear, then the volume of material is sputtered. Theoretically a hemispherical sputtered volume is predicted.[12–14] At the extremities of the crater, the surface material does not receive enough momentum to escape, but as more highly energized underlying material attempts to eject, a plastic surface deformation in the form of a bulge or rim is induced. A similar scenario occurs for a grazing incidence ion (Fig. 5, bottom). Here the force per unit volume is directed nearly normal to the surface. At points for which the ion track is close to the surface, material receiving more than the critical impulse can easily escape, leading to sputtering. However, at locations where the ion track is deeper, material receiving the critical impulse is impeded by the stationary material above. The result is a tail-like plastic deformation along the ion track.

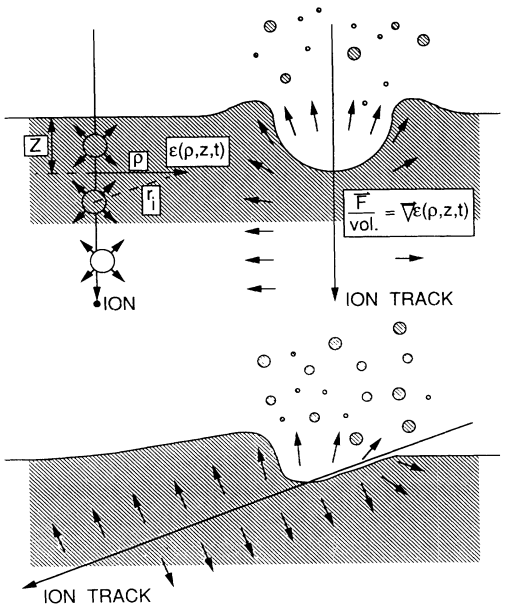

FIG. 5. Schematic diagram of models of sputtering and plastic deformation due to a cylindrical pressure pulse. See the text for details.

For solid leucine (MW 131 u), the sputtering yield of neutral molecules scales as the third power of electronic stopping cross section,[26] in agreement with the pressure pulse model.[12] However, for solid valine, monomer ion ejection patterns show a normally directed near-cosine thermal-type distribution,[27] inconsistent with both off-normal ejection patterns predicted by the pressure pulse model[12–14] and observed for larger sputtered organics.[28] We, nonetheless, observe in ion-bombarded valine, clear evidence for a correlated volume force due to a pressure pulse emanating from the ion track. This pulse probably plays a dominant role in causing the large yield of sputtered neutral particles.[4]

In conclusion, scanning force microscopy has provided a new and unique view of the intersection of an ion track with a surface and has elucidated the response of a material to a dense microscopic track of deposited energy. Further studies are planned to determine crater morphology as a function of ion stopping power, ion charge state, and target composition.

The authors thank the Swedish Research Council for Engineering Sciences (TFR), the Swedish National Science Research Council (NFR), the Swedish Biomaterial Consortium funded by the Swedish National Board for Industrial and Technical Development (NUTEK), and the Göran Gustafsson Foundation. We also thank P. Demirev, N. Keskitalo, and G. Brinkmalm for occasional assistance with sample bombardments and P. Håkansson, R. E. Johnson, and D. Fenyö for helpful discussions.

[1]J. P. Bradley, D. E. Brownlee, and P. Fraundorf, Science **226**, 1432 (1984).
[2]M. A. Kadhim *et al.*, Nature (London) **355**, 738 (1992).
[3]R. L. Fleischer, P. B. Price, and R. M. Walker, *Nuclear Tracks in Solids* (University of California, Berkeley, 1975).
[4]M. Salehpour *et al.*, Nucl. Instrum. Methods B **13**, 278 (1986).
[5]B. U. R. Sundqvist and R. D. Macfarlane, Mass Spectrom. Rev. **4**, 421 (1985).
[6]P. Håkansson, Det Kgl. Danske Videnskab. Selskab Mat. Fys. Medd. **43** (to be published).
[7]C. T. Reimann, Det Kgl. Danske Videnskab. Selskab Mat. Fys. Medd. **43** (to be published).
[8]P. Williams and B. U. R. Sundqvist, Phys. Rev. Lett. **58**, 1031 (1987).
[9]R. D. Macfarlane and D. F. Torgerson, Science **191**, 920 (1976).
[10]R. R. Lucchese, J. Chem. Phys. **86**, 443 (1987).
[11]R. E. Johnson, and B. U. R. Sundqvist, Phys. Today **28**, (3) (1992).
[12]R. E. Johnson *et al.*, Phys. Rev. B **40**, 49 (1989).
[13]D. Fenyö and R. E. Johnson, Phys. Rev. B **46**, 5090 (1992).
[14]D. Fenyö *et al.*, Phys. Rev. B **42**, 1895 (1990).
[15]I. S. Bitensky and E. S. Parilis, Nucl. Instrum. Methods B **21**, 26 (1987).
[16]S. Manne *et al.*, J. Cryst. Growth **130**, 333 (1993).
[17]M. J. Allen *et al.*, Ultramicroscopy **42-44**, 1095 (1992).
[18]I. V. Vorob'eva and E. A. Ter-Ovanes'yan, Fiz. Tverd. Tela (Leningrad) **34**, 414 (1992) [Sov. Phys. Solid State **34**, 222 (1992)].
[19]F. Thibaudau *et al.*, Phys. Rev. Lett. **67**, 1582 (1991).
[20]P. Bauer *et al.*, Europhys. Lett. **23**, 585 (1993).
[21]J. Ackermann *et al.*, Radiat. Eff. **126**, 213 (1993).
[22]D. Snowdon-Ifft *et al.*, Phys. Rev. Lett. **70**, 2348 (1993).
[23]G. Säve *et al.*, Appl. Phys. Lett. **51**, 1379 (1987).
[24]G. Bolbach *et al.*, Rap. Commun. Mass Spectrom. **1**, 22 (1987).
[25]R. Schmidt *et al.*, Phys. Rev. B **44**, 560 (1991).
[26]A. Hedin *et al.*, Phys. Rev. B **35**, 7377 (1987).
[27]R. Moshammer *et al.*, in *Ion Formation from Organic Solids (IFOS V)*, edited by A. Hedin, B.U.R. Sundqvist, and A. Benninghoven (Wiley, New York, 1990), p. 17.
[28]W. Ens *et al.*, Phys. Rev. B **39**, 763 (1989).

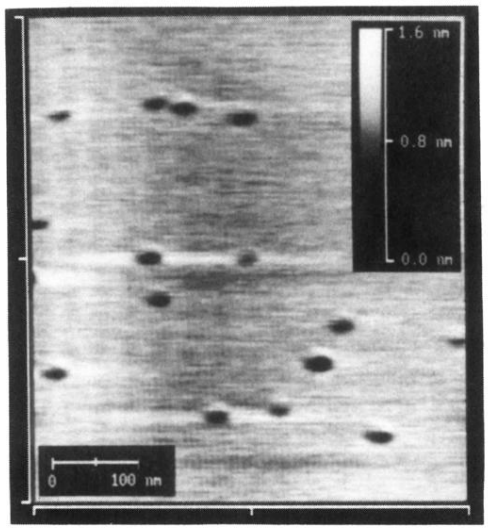

FIG. 1. Continuous contact mode SFM image of single-crystal *L*-valine irradiated at normal incidence by 78.2-MeV ^{127}I ions. Some distortion due to tip-surface interactions is apparent.

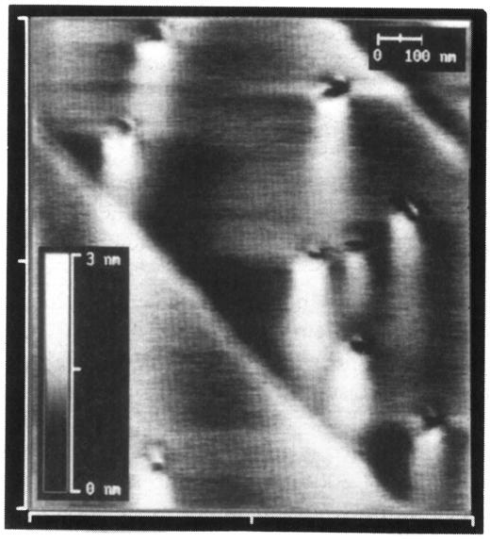

FIG. 2. Continuous contact mode SFM image of single-crystal *L*-valine irradiated at a 79° grazing angle of incidence. The tail is smooth as evidenced by the preserved step edge seen crossing one of the tails.

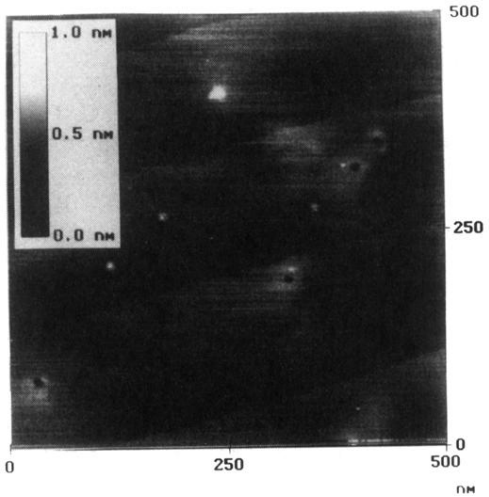

FIG. 3. Tapping mode SFM image of single-crystal *L*-valine irradiated at normal incidence.

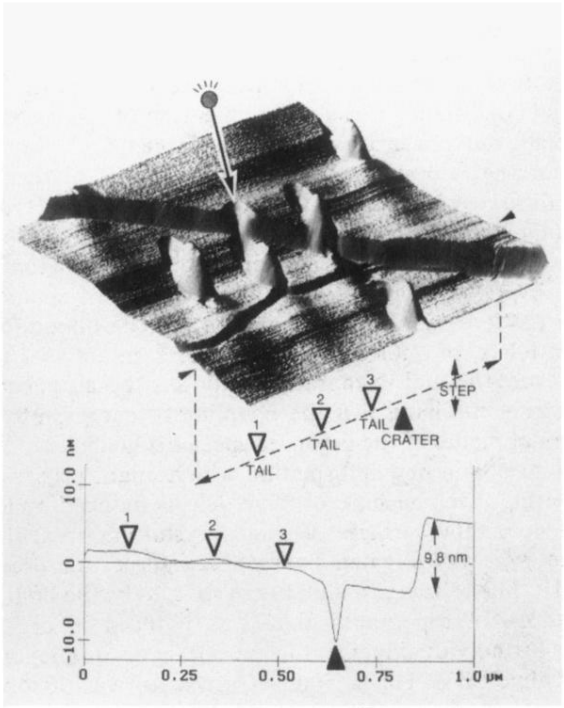

FIG. 4. Tapping mode SFM image of single-crystal *L*-valine irradiated at grazing incidence. The direction of the incident ions is shown schematically (note that the vertical scale differs from the horizontal scale). The scan area is 1000 nm × 1000 nm. The dominant step edge is 9.8 nm tall and corresponds closely to eight crystal planes (Ref. 16). A profile scan of three of the tails is shown.

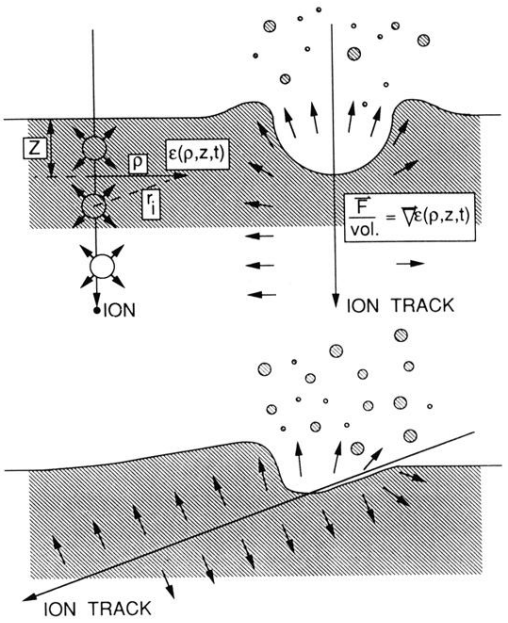

FIG. 5. Schematic diagram of models of sputtering and plastic deformation due to a cylindrical pressure pulse. See the text for details.